



Assessment of computational weld mechanics concepts for estimation of residual stresses in welded box structures

Downloaded from: <https://research.chalmers.se>, 2024-05-01 23:46 UTC

Citation for the original published paper (version of record):

Zhu, J., Khurshid, M., Barsoum, Z. (2019). Assessment of computational weld mechanics concepts for estimation of residual stresses in welded box structures. *Procedia Structural Integrity*, 17: 704-711.
<http://dx.doi.org/10.1016/j.prostr.2019.08.094>

N.B. When citing this work, cite the original published paper.



ICSI 2019 The 3rd International Conference on Structural Integrity

Assessment of computational weld mechanics concepts for estimation of residual stresses in welded box structures

J. Zhu^{a,*}, M. Khurshid^{a,b}, Z. Barsoum^{a,c}

^a*KTH Royal Institute of Technology, Teknikringen 08, Stockholm 10044, Sweden*

^b*Cargotec Sweden AB Bromma Conquip, Kronborgsgränd 23, Kista 16446, Sweden*

^c*Chalmers University of Technology, Chalmersplatsen 4, Gothenburg 41296, Sweden*

Abstract

In this study finite element simulation approaches (lumping and prescribed temperature) are implemented to study residual stress distribution in a welded box type structure. This component is a vital part in several load carrying structural applications and the residual stresses are important to quantify from a structural integrity point of view. The thermal history from simulations has been verified with experimental measurements. The residual stresses at the weld toe side were measured, using X-ray diffraction technique. It is shown that a similar trend of residual stress state was captured by the simulation, compared to experimental measurements. The estimated residual stresses from the cases of welds with full penetration and partial penetration are slightly different along the crack path. Compressive residual stress was near the area of both weld toe and root while tensile residual stress was in the center of the weld with the magnitude up to 820 MPa. Moreover, a sub model of the welded box type structure is studied using the following computational weld mechanics concepts: Thermo-elastic-plastic, lumping and prescribed temperature, in order to assess the computational time and the magnitude of estimated residual stresses.

© 2019 The Authors. Published by Elsevier B.V.
Peer-review under responsibility of the ICSI 2019 organizers.

Keywords: Finite element method; residual stresses; welding simulation; welded box structures;

* Corresponding author. Tel.: +46 70 087 7097.
E-mail address: jinchao@kth.se

1. Introduction

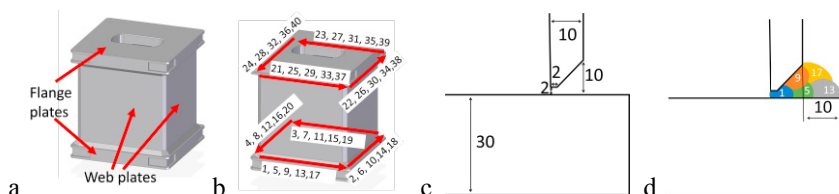
Arc welding is one of the most common joining methods in the steel construction industry. Welding-induced residual stresses occur as a result of shrinkage in the weld metal and the restraints of its adjacent base metal during cooling. These stresses have a vital effect on the fracture and fatigue behaviors of the welded structures subject to dynamic loading (Feng (2005)). Thus, it is of significant importance to quantify welding residual stresses from a structural integrity point of view.

A number of computational welding mechanics (CWM) methods have been developed over the last few decades. The Thermo-elastic-plastic method has been widely applied to different types of small welded structures such as butt welds (Long H et al. (2009)), fillet welds (Teng TL et al. (2001)) and overlap welds (Schenk T et al. (2009)), because of its high accuracy. However, the application of the Thermo-elastic-plastic method on large welded structures is limited by the high level of computational time required. Thus, it is essential to develop and implement different numerical techniques for increasing the computational efficiency. Lindgren et al. (1999) used the prescribed temperature method as a means for heat input to study the residual stress state as a result of multipass butt welding of a very thick plate. Yang et al. (2002) developed a lump-pass weld simulation technology for shipbuilding to predict and control distortion and residual stresses, in order to reduce the number of weld passes. Khurram et al. (2012) investigated an efficient FE technique based on inherent strain named equivalent load to predict welding deformations and residual stresses in butt joints. The equivalent load is calculated by integration of inherent strain which is a function of the highest temperature and degree of restraint. Zhu et al. (2019) compared the Thermo-elastic-plastic, inherent strain (local-global) and substructuring methods to predict weld distortion and residual stress state of T-type fillet weld and multi-pass butt weld and they concluded the inherent strain (local-global) method is very time-efficient and the estimated longitudinal residual stresses show good agreement with the experimental measurements.

In this study, the finite element simulation using lumping method, together with prescribed temperature method, is implemented on welded box structures to estimate welding residual stress state. The simulations have been performed using commercial software: SYSWELD. The welded box type structures studied have fully penetrated and partially penetrated welds. The thermal history from simulations has been verified with experimental measurements. Residual stress measurements at the weld toe side were carried out by X-ray diffraction technique. Moreover, a sub model of the welded box type structure is studied using the following computational weld mechanics concepts: Thermo-elastic-plastic, lumping and prescribed temperature, in order to assess the computational time and the magnitude of estimated residual stresses of those concepts.

2. Box welded structure

The welded box type structure consisted of two flanges (Structural steel of S700 grade) with a thickness of 30 mm which have a hole in the center of the plate, and four web plates (Structural steel of S600MC grade) with a thickness of 10 mm, see Fig. 1a. Before welding, the plates were tack welded together at the corners and afterwards the tack welds were grinded. The welds were produced manually using Metal Active Gas (MAG) with the multi-pass process (5 passes). A total of 8 multi-pass welds are included in the structure. The total number of weld passes is 40. Fig. 1b illustrates the weld sequence. The dimension of weld groove can be seen in Fig. 1c. Fig. 1d shows the deposition of weld passes numbering 1, 5, 9, 13 and 17, which is the same for the other multi-pass welds.



The welding parameters of 5 passes can be seen in Table 1. No external constraint was applied to the welded box structures during the manufacturing process. A wire brushing operation was carried out after welding process to clean the welded box type structure.

Table 1. Welding parameters

Pass number	Wire size (mm)	Wire feed speed (m/min)	Current (amp)	Voltage (volts)	Welding speed (mm/s)
1	1.2	3	123-138	19-20	2.5
2	1.2	3	206-215	21-22	6
3	1.2	5	195-213	21-22	6
4	1.2	9.4	257-271	23-24	5.5
5	1.2	9.4	257-271	24-25	5.7

3. Experiments

3.1. Temperature measurements

During the experiment, temperature data was collected using K-type thermocouples. A hole with a diameter of 3 mm and a depth of 2 mm was drilled to insert the thermocouples which are 10 mm from the edge of the plate, as shown in Fig. 2.

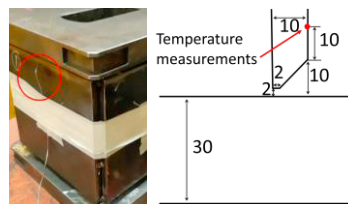


Fig. 2. Temperature measurement;

3.2. Residual stress measurements

The residual stresses were measured using the X-ray diffraction method with Cr $K\alpha$ radiation. Table 2 shows the used X-ray diffraction parameters. The first measuring point was taken at 2 mm from the weld toe and the distance between measuring points was 4 mm, see Fig. 3.

Table 2. X-ray diffraction parameters

Voltage	Current	X-ray diffraction planes	Collimator
30 kV	1.6 mA	$2\theta=156.4^\circ$	4 mm

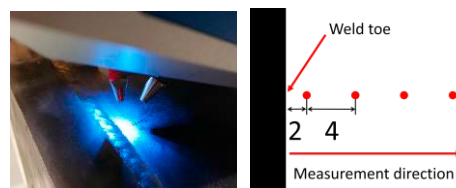


Fig. 3. Residual stress measurements;

3.3. Macrographs

The macrographs at the steady state part of the welds were made, with grinding and polishing to 1 μm diamond size followed by etching with 2% Nital. Fig. 4 shows the fully penetrated and partially penetrated welds. It is observed that the weld in Fig. 4b has approximately 2 mm lack of penetration which is defined as the case of partial penetration.

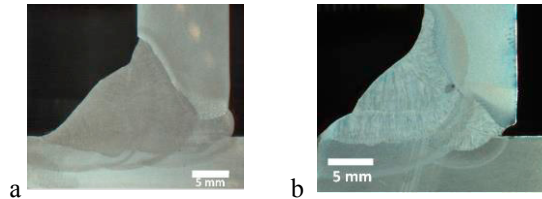


Fig. 4. (a) Full penetration; (b) Partial penetration;

4. Finite element analysis

4.1. Computational welding mechanics methods

Finite element simulation using the lumping method, together with prescribed temperature method, is implemented on the welded box structure to estimate welding residual stress state. The lumping method could reduce the number of weld passes by lumping several weld passes into one large pass. The heat input and welding speed of the large pass need to be calibrated based on temperature measurements and macrographs (Yang et al. (2002)); see Section 4.2. In the prescribed temperature method, the prescribed temperature curve was calculated from Thermal-elastic-plastic method using a moving heat source. The temperature history of the nodes in the molten zone was averaged. Afterwards, the averaged temperature history curve was applied on the entire weld bead assuming the infinite welding speed in the sequential thermomechanical welding simulation, see Section 4.2 and 4.3.

4.2. Thermal analysis

Bhatti et al. (2015) reported that except yield stress, all of the thermo-mechanical properties could be considered as constant, which gave acceptable accuracy of the estimation of residual stresses. Furthermore, the difference between the temperature dependent yield stresses of the same steel grade is quite small (Bhatti et al. (2015)). Thus, the thermal-physical properties with considering phase transformation of TRIP700Z and DP-W-600 in material database of SYSWELD were used as material model of flange plates and filler material having yield strength at 700 MPa and web plates having yield strength at 600 MPa.

In the lumping analysis, the five weld passes were lumped into two weld passes, which reduces the total number of weld passes from 40 to 16. The first three weld passes were lumped into one pass defined as lump-pass 1 and the last two passes were lumped into another pass defined as lump-pass 2, as shown in Fig. 5.

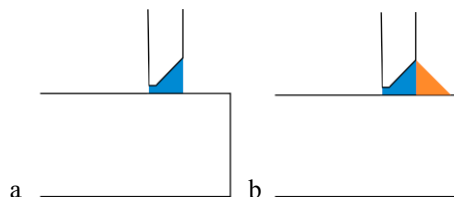


Fig. 5. (a) Lump-pass 1; (b) Lump-pass 2;

The total heat input of lump-pass weld in which n weld passes are lumped is shown in Equation 1.

$$Q = \eta \sum_{1}^n U_n I_n \quad (1)$$

In the equation 1, η is welding efficiency, U is voltage and I is current. The efficiency η and the welding speed of lump-pass were calibrated based on the temperature measurements. The moving welding arc was modeled as the double ellipsoid distribution developed by Goldak (Goldak et al. (1984)), where a_f is the forward length, a_r is the rear length, b is the width and c is the depth of the heat source. The parameters of double ellipsoid model were calibrated according to the match between the macrographs and the isothermal contour plots for the fusion zone. Table 3 shows the parameters of the welding efficiency and speed and the double-ellipsoidal heat source model for the lump-pass 1 and 2.

Table 3. Heat source parameters

Lump-pass weld number	Welding speed (mm/s)	Efficiency η	a_f	a_r	b	c
1	6	0.55	5	10	5	11
2	5.6	0.6	5	10	7	8

The results from the thermal analysis for the two lump-pass welds are presented in Fig. 6. The fusion zones in the isothermal contour plots and macrographs match well, see Fig. 6a. The values of peak temperature of the weld passes numbering 1, 5 and 13 are lower than the ones of weld passes numbering 9 and 17 since the location of weld passes numbering 9 and 17 is close to the temperature measurement point. Therefore, the temperature curves from lump-pass welds have been calibrated according to the temperature measurement of weld passes 9 and 17, see Fig. 6b.

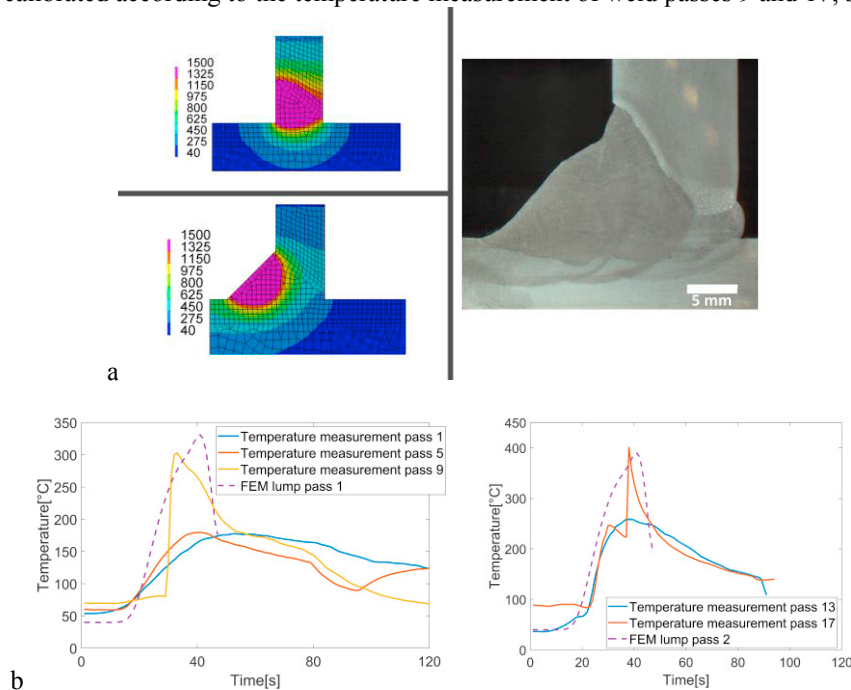


Fig. 6. (a) Fusion zone and isotherms; (b) Experimental and numerical temperature history;

In the prescribed temperature analysis, the temperature curves of all the nodes in the molten zone with temperatures equal or above 1500°C were averaged and made into the prescribed temperature curve which is shown in Fig. 7a. The prescribed temperature curve was applied on all the nodes associated with a weld. This corresponds to the weld with infinite welding speed, as shown in Fig.7b.

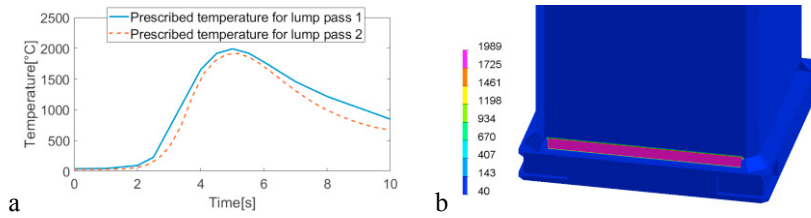


Fig. 7. (a) Prescribed temperature for lump pass 1 and 2; (b) Temperature distributions

4. Mechanical analysis

The rigid body motion was prevented due to no external constraint added to welded box structures during the manufacturing process. The length of elements in the weld beads were set at 2 mm for all the passes. The coarse mesh was applied to the region far away from the welds with the value of 10 mm. The total number of elements was 500000 and the simulation time of using 8 cores is 21 hours.

Fig. 8 shows the comparison of experimental and estimated residual stresses in Z direction in front of the weld toe. According to the surface residual stress measurements, the compressive residual stresses were found with the magnitude between 316 MPa and 463 MPa. The estimated residual stresses from the cases of welds with full penetration and partial penetration are similar, which show tensile residual stresses up to 200 MPa. The difference between the numerical results and experimental measurements can be attributed to that the wire brushing operation could generate the near-surface compressive residual stresses with the magnitude up to 500 MPa, which was reported by Rhouma et al. (Rhouma et al. (2001)). However, a similar trend of residual stresses is observed in both experimental measurements and simulations. In order to increase the accuracy of simulation, the numerical simulation of wire brushing operation could be included in further studies. Furthermore, the epistemic uncertainty related to residual stress measurement can also be quantified (Sandberg et al. (2017)). However, more experimental data will be needed.

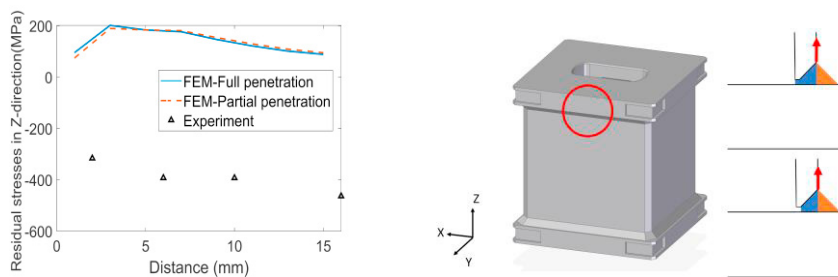


Fig. 8. Residual stresses along Z direction at weld toe

The estimated residual stresses in Z direction along the path from the weld toe to weld root can be seen in Fig. 9. In the x axis, the position of 0 mm is corresponding to weld toe. The residual stress of the weld with partial penetration shows compressive (-45 MPa) at the weld root (x=17 mm). The tensile residual stress (6 MPa) is found at the weld root (x=19 mm) of the weld with full penetration. However, the difference between the estimated residual stresses from the fully penetrated and partially penetrated welds are small. It is shown that the residual stresses near both weld

toe and root side are compressive and the residual stresses in the center of the weld are tensile with the magnitude up to 820 MPa. A similar residual stress state was observed in the simulation of multi-pass welded tubular structures carried out by Barsoum (Barsoum Z. (2007)).

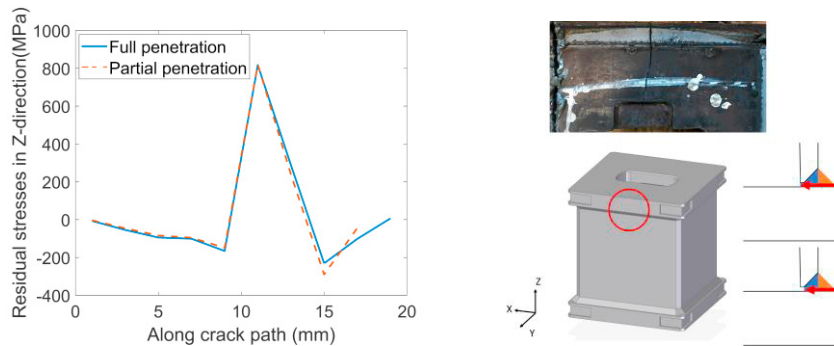


Fig. 9. Residual stresses along Z direction along crack path

5. Discussion

In order to assess the following computational weld mechanics concepts: Thermo-elastic-plastic, lumping and prescribed temperature, in terms of the computational time and the magnitude of estimated residual stresses, we studied a sub model of the welded box type structure with a fully penetrated weld having three weld passes numbering 1, 5 and 9, as shown in Fig. 10. The length of the weld is 100 mm. The total number of 3D elements is 68650 and the number of CPU cores is 8.

The prescribed temperature method (3718s) reduces computational time by approximately 80%, compared to the Thermo-elastic-plastic method (16964s). The computational time for using lumping method, together with prescribed temperature method (1317s) is 65% less than the prescribed temperature method. The maximum estimated residual stresses in Z direction in front of the weld root are compared. Fig. 10 shows that the residual stress calculated using prescribed temperature method is 119 MPa which is 67% less than that of the Thermo-elastic-plastic method (359 MPa). This is due to the fact that the effect of constraints on the colder regions in front of and after the arc in the prescribed temperature method is less than the one from the thermo-elastic-plastic method using a moving heat source (Lindgren, LE. (2001)). The residual stress calculated using lumping method together with prescribed temperature method (192 MPa) is 46% less than that of the Thermo-elastic-plastic method. Therefore, the magnitude of residual stresses may be underestimated.

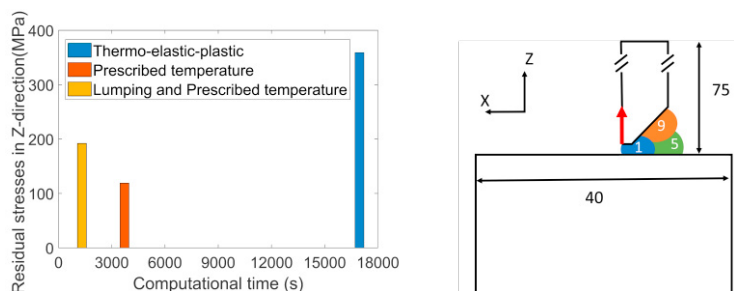


Fig. 10. Computational time and estimation residual stresses

Conclusion

1. The prescribed temperature method can reduce the computational time by 80% as compared to the Thermo-elastic-plastic method. Furthermore, the computational time for using lumping method, together with prescribed temperature method is 65% less than the prescribed temperature method. However, the magnitude of residual stresses may be underestimated.
2. According to the residual stress state along the crack path, it is found that the residual stresses near both weld toe and root side are compressive which contribute to the closure of the crack. However, the residual stresses in the center of the weld are tensile with the magnitude up to 820 MPa which contribute to the opening of the crack.
3. It is shown that the estimated residual stresses from the cases of welds with full penetration and partial penetration are slightly different.
4. A similar trend of the residual stress state in front of the weld toe is observed in the experimental measurements using X-ray diffraction technique and simulations using lumping method, together with prescribed temperature method.

Acknowledgements

The members of the project Reduced variation in the manufacturing processes enabling lightweight welded structures VariLight (Sweden's Innovation Agency VINNOVA, Grant Number 2016-03363) is gratefully acknowledged for their support. Schlumpf Scandinavia AB and Stresstech Oy are thanked for their help in making residual stresses measurement in welded box structures. ESI Group is acknowledged for their support in the software SYSWELD.

References

- Feng, Z. ed., 2005. Processes and mechanisms of welding residual stress and distortion. Elsevier, pp. 3.
- Long, H., Gery, D., Carlier, A. and Maropoulos, P.G., 2009. Prediction of welding distortion in butt joint of thin plates. *Materials & Design*, 30(10), pp.4126-4135.
- Teng, T.L., Fung, C.P., Chang, P.H. and Yang, W.C., 2001. Analysis of residual stresses and distortions in T-joint fillet welds. *International Journal of Pressure Vessels and Piping*, 78(8), pp.523-538.
- Schenk, T., Richardson, I.M., Kraska, M. and Ohnimus, S., 2009. Modeling buckling distortion of DP600 overlap joints due to gas metal arc welding and the influence of the mesh density. *Computational Materials Science*, 46(4), pp.977-986.
- Lindgren, L.E., Runnemalm, H. and Näsström, M.O., 1999. Simulation of multipass welding of a thick plate. *International journal for numerical methods in engineering*, 44(9), pp.1301-1316.
- Yang, Y.P., Brust, F.W. and Kennedy, J.C., 2002, January. Lump-pass welding simulation technology development for shipbuilding applications. In *ASME 2002 Pressure Vessels and Piping Conference* (pp. 47-54). American Society of Mechanical Engineers.
- Khurram, A. and Shehzad, K., 2012. FE simulation of welding distortion and residual stresses in butt joint using inherent strain. *International Journal of Applied Physics and Mathematics*, 2(6), p.405.
- Zhu, J., Khurshid, M. and Barsoum, Z., 2019. Accuracy of computational welding mechanics methods for estimation of angular distortion and residual stresses. *Welding in the World*, DOI: 10.1007/s40194-019-00746-9.
- Bhatti, A.A., Barsoum, Z., Murakawa, H. and Barsoum, I., 2015. Influence of thermo-mechanical material properties of different steel grades on welding residual stresses and angular distortion. *Materials & Design* (1980-2015), 65, pp.878-889.
- Goldak, J., Chakravarti, A. and Bibby, M., 1984. A new finite element model for welding heat sources. *Metallurgical transactions B*, 15(2), pp.299-305.
- Rhouma, A.B., Sidhom, H., Braham, C., Lédion, J. and Fitzpatrick, M.E., 2001. Effects of surface preparation on pitting resistance, residual stress, and stress corrosion cracking in austenitic stainless steels. *Journal of materials engineering and performance*, 10(5), pp.507-514.
- Sandberg, D., Mansour, R., and Olsson, M., 2017. Fatigue probability assessment including aleatory and epistemic uncertainty with application to gas turbine compressor blades. *International Journal of Fatigue*, 95, 132-142.
- Barsoum, Z., 2007. Residual stress prediction and relaxation in welded tubular joint. *Welding in the World*, 51(1-2), pp.23-30.
- Lindgren, L.E., 2001. Finite element modeling and simulation of welding part 1: increased complexity. *Journal of thermal stresses*, 24(2), pp.141-192.